Zoological Journal of the Linnean Society, 2007, **150**, 895–914. With 7 figures

Postcranial element shape and function: assessing locomotor mode in extant and extinct mustelid carnivorans

HEIDI SCHUTZ* and ROBERT P. GURALNICK

Department of Ecology and Evolutionary Biology, University of Colorado, Boulder, CO 80309, USA

Received November 2005; accepted for publication December 2006

Assessment of locomotor modes in fossil taxa must often be made on the basis of heavily fragmented postcranial material. Previous authors have used quantitative methods to determine locomotor function from whole postcranial elements. The goals of this project were to assess the ability of element shape to discern between locomotor modes through landmark analysis, and to apply the results to assessment of fossils. Results suggest that element shape is a good predictor of function, but that different elements have different predictive capacities for each locomotor mode. Additionally, a relationship between size and shape exists that appears to drive morphological differentiation in the group. Finally, data from the extant sample were applied to fossil material of the extinct Plio-Pleistocene taxon *Trigonictis*. The results suggest that the locomotor mode of *Trigonictis* was generalized and probably an intermediate between the half-bound locomotion found in weasels and ferrets and the scansorial locomotion of martens and fishers.

ADDITIONAL KEYWORDS: canonical variates analysis – Carnivora – geometric morphometrics – locomotion – Mammalia, Mephitidae functional morphology – multivariate statistics – Mustelidae.

INTRODUCTION

Assessment of function from skeletal material in the mammalian fossil record depends on two factors: the relevance of comparisons between fossil and extant lineages, and the abundance and quality of information extractable from the available fossil material. In this study, we use geometric morphometrics as a means to produce inferences regarding the form and function of fossil material by considering them in the context of a large database of modern forms.

Our approach follows a long tradition of morphological examination of function where, historically, researchers used either detail-rich qualitative analyses (Taylor, 1974, 1976) or statistically relevant quantitative approaches (e.g. Van Valkenburgh, 1987; MacLeod & Rose, 1993). In particular, the work of Van Valkenburgh (1987) and later that of MacLeod & Rose (1993) illustrated the way in which qualitative and quantitative approaches can be combined in order to quantify shape. They developed morphospaces, based on extant organisms, then projected fossil specimens onto those morphospaces. Van Valkenburgh (1987) created a database of morphological indices for carnivores with known locomotor modes and used multivariate classification approaches to determine whether those indices predicted locomotor categories. She then projected fossil elements onto an extant shape space to determine their correspondence to modern groups. MacLeod & Rose (1993) utilized eigenshape analysis to quantify measures of shape for terminal phalanges and proximal radial heads. They then used these measures to infer locomotor behaviour in modern and Paleogene mammals.

More recently, other researchers have incorporated these geometric morphometric approaches to studies of functional morphology. Bonnan (2004) combined a landmark-based approach with linear measures to assess possible locomotor differences between sauropod dinosaurs. Andersson's (2004) landmark analyses examined the articular surface of the distal

*Corresponding author. E-mail: heidi.schutz@colorado.edu

humerus in carnivorans that employ either stalk/ambush or sustained pursuit predatory strategies. He found that although an ecomorphological continuum exists the two functional modes are discernible when distal humerus articular shape is examined.

In this study, we also use landmark-based analyses of shape to predict function, focusing on a smaller, yet functionally diverse clade of carnivores – the musteloids (e.g. badgers, weasels, skunks, raccoons and lesser pandas). First, we generated a set of landmark-based shape descriptors for fossil and extant mustelids and mephitids. Second, because locomotor adaptations in an organism are not inherently global, but more probably localized in the regions most active during any given locomotor activity, we utilized a multi-appendicular element approach similar to that of Holmes (1980), allowing us to incorporate a more complete view of the skeletal locomotor apparatus in this group of carnivores that possesses so much functional diversity relative to other families in the order. Third, we used these shape descriptors along with information about locomotor behaviour to asses our ability to discern locomotor function of extant musteloids and then of the fossil genus *Trigonictis*. Consequently, our examination of multiple skeletal elements produces a broader picture of the morphological shifts associated with a given functional regime.

MUSTELID CARNIVORES

The family Mustelidae provides an excellent model for examining postcranial form and locomotor function within the order Carnivora because of its locomotor diversity. In a study of linear measurement ratios and qualitative comparisons of the appendicular skeleton of mustelids (including mephitids), Holmes (1980) concluded that a continuum of specialization in locomotor mode exists within the family. This continuum includes fossorial, arboreal, cursorial, aquatic and ambulatory modes of locomotion, representing increasing levels of specialization accompanied by corresponding levels of morphological disparity. Although Holmes (1980) concluded that the continuum also reflects in part morphological generalization within the Mustelidae, his results also confirmed the existence of significant morphological differences between locomotor groups. Additionally, Holmes (1980) and Simpson (1945) suggested that these locomotor modes closely follow phylogenetic relationships of the Mustelidae, implying that postcranial morphology in this group may be utilized both to infer locomotor mode and potentially identify taxa.

Recently there have been substantial changes in our understanding of the phylogeny of musteloid carnivores (Bryant, Russel & Fitch, 1993; Dragoo & Honeycutt, 1997; Bininda-Emonds, Gittleman & Purvis, 1999; Flynn *et al*., 2000; Koepfli & Wayne, 2003). These new studies now suggest that skunks constitute their own monophyletic clade, the Mephitidae, a sister family to the Mustelidae. Both groups are part of a broader clade Musteloidea that also includes raccoons and lesser pandas (Dragoo & Honeycutt, 1997; Flynn *et al*., 2000). However, within this broader musteloid lineage, the patterns observed by Holmes (1980) and Simpson (1945) still remain relevant.

Background on the fossil taxon Trigonictis: Mustelid-like carnivores can be traced back to early Oligocene weasel- and badger-like forms. However, not until the early Miocene of North America and Eurasia do we see the emergence of the major mustelid radiations. By the late Miocene, most genera of true mustelids had emerged (Martin, 1989).

The extinct genus *Trigonictis* is found in North American Pliocene and Pleistocene deposits and is regarded by Kurtén & Anderson (1980) as living in a variety of habitats and as capable of climbing and swimming. Currently represented by two species, *Trigonictis macrodon* (formerly *idahoensis*) and *T. cookii*, this genus is largely known from Blancan deposits (Ray, Anderson & Webb, 1981).

Various workers (Gazin, 1934; Zakrzewski, 1967; Bjork, 1970; Ray *et al*., 1981; Anderson, 1989; Martin, 1989) examined the possible phylogenetic associations of *Trigonictis* within the Mustelidae. Gazin (1934) considered *Trigonictis* to be closely related to the genus *Galictis* based on similarities in dental morphology. Ray *et al*. (1981) re-examined the same material and suggested a closer dental affinity to *Eira* (also considered a member of the Galictinae at the time), but also found similarities to *Galictis*, and concluded that *Trigonictis* was ancestral to both genera.

Galictis is highly terrestrial and resembles skunks behaviourally and morphologically. *Eira*, by contrast, resembles the highly arboreal martens and fishers. These differences, as well as recent mustelid phylogenies that include both *Galictis* and *Eira* (Bryant *et al*., 1993; Bininda-Emonds *et al*., 1999; Koepfli & Wayne, 2003), challenge the existence of the Galictinae as a clade. More probably, *Eira* is a member of a robust marten (*Martes*) and wolverine (*Gulo*) clade while *Galictis* is a sister genus to the *Mustela* clade. These data further complicate previous assessments of *Trigonictis*.

The goals of this study were to apply landmark-based morphometric analyses to functional predictions of modern and fossil materials. Specifically, we used these methods to test the following hypotheses and predictions:

Hypothesis 1. Significant differences exist in the postcranial element shape of mustelid locomotor groups.

Prediction 1. Sufficient differentiation exists in the morphology of musteloid appendicular elements to infer locomotor mode and functional morphology of extant lineages.
Prediction 2. The ability of elements to differentiate between locomotor groups is not uniform across elements and some elements differentiate certain groups better than others.
Hypothesis 2. Contrary to what would be expected from previous work, *Trigonictis* does not share the same locomotor mode as either *Eira* or *Galictis*.

MATERIAL AND METHODS

MATERIAL

Sixteen species of the family Mustelidae, two species of the family Mephitidae (Dragoo & Honeycutt, 1997; Flynn *et al*., 2000) and fossil representatives of the genus *Trigonictis* were examined in this study (Appendix 1).

Both males and females were included in the study as well as individuals of unknown sex when preliminary analyses showed no sexual shape differences in these appendicular elements. Only mature specimens were sampled; maturity was determined on the basis of closure of cranial sutures, emergence of molars and fusion at epiphyses. The exclusion of immature specimens greatly limited sample size. However, the omission was considered necessary because preliminary analyses suggested the existence of significant age-related shape differences.

Two criteria for data collection – sample quality and functional significance – were used in this study. The most plentiful and best preserved postcranial elements for the extinct genus *Trigonictis* were chosen. The regions within those elements that provided optimal morphological information with regard to function (i.e. well-preserved articular surfaces and sites for muscle attachment) were then landmarked. Using these criteria, the following elements and regions were chosen for this study: humeral distal extremity, cranial aspect (Fig. 1A, Table 1A); ulnar proximal extremity, dorsal aspect (Fig. 1B, Table 1B); femoral proximal extremity, caudal aspect (Fig. 1C, Table 1C); complete tibia, cranial aspect (Fig. 1D, Table 1D). Landmarking of the first three elements focused on the dense proximal and distal extremities. The fourth element was used in its entirety because of the exceptional preservation present in all of the *Trigonictis* tibiae.

METHODS

Data collection

Landmarks were recorded as two-dimensional Cartesian coordinates on high-resolution digital images utilizing TpsDig software written by F. J. Rohlf (http://life.bio.sunysb.edu/morph/). Landmarks were selected based on their ability to capture both morphological variability and features related to different functional adaptations. Thus, many of the landmarks were placed at sites of critical muscle attachments and regions of articulation between elements that were for the most part identifiable and repeatable anatomical landmarks. Landmark placement and justification is detailed in Figure 1A–D and Table 1A–D. For example, in the humerus, landmarks 1, 2 and 10 (Fig. 1A) sample the region of the medial epicondyle, a site of attachment for pronators of the forearm and wrist flexors. In the femur, landmarks 1–3 and 10 (Fig. 1D) sample the femoral head that articulates with the acetabulum on the os coxae.

A Generalized Least Squares Procrustes Fit was performed on the raw landmark data and then a thin-plate spline function was used for interpolating change between landmarks (Bookstein, 1991). These local and global shape differences are represented

Table 1A. Landmark descriptions and configuration: humerus (*Martes pennanti* as representative species)

Landmark	Description
1.	Ulnar groove at the point of junction with the distal humeral articular surface
2.	Maximum distal projection of the trochlea
3.	Maximum proximal curvature of the distal edge of the trochlea
4.	Junction point between capitulum and lateral epicondyle
5.	Maximum lateral curvature of lateral epicondyle
6.	Maximum lateral projection of lateral epicondylar ridge
7.	Junction point between lateral epicondylar ridge and humeral shaft
8.	Point directly opposite landmark 7 on medial side
9.	Point of change in curvature between the humeral shaft and the medial epicondyle
10.	Medialmost projection of the medial epicondyle
11.	Maximum distal projection of proximal edge of trochlea

Table 1B. Landmark descriptions: ulna (*Martes pennanti* as representative species)

Landmark	Description
1.	Distalmost projection of lateral edge of olecranon process
2.	Absolute distalmost projection of olecranon process on distal edge
3.	Distalmost projection of medial aspect of olecranon process
4.	Midpoint between landmarks 3 and 5 on the cranial ridge of the olecranon
5.	Medialmost projection of distal ridge of trochlear notch
6.	Lateralmost curvature of trochlear notch
7.	Medialmost projection of the proximal ridge of trochlear notch
8.	Curvature change between trochlear notch and ulnar shaft on medial side
9.	Proximalmost point of coronoid process at the endpoint of the ulnar tuberosity
10.	Lateralmost point of radial notch at transition with trochlear notch.
11.	Medialmost curvature of trochlear notch.
12.	Lateralmost projection of distal ridge of trochlear notch
13.	Midpoint between landmarks 1 and 12.

Table 1C. Landmark descriptions: femur (*Martes pennanti* as representative species)

Landmark	Description
1.	Fovea capitis on lateral edge of femoral head
2.	Proximalmost projection of femoral head
3.	Transition on proximal edge between articular surface of head and femoral neck
4.	Point of transition between the greater trochanter and the femoral neck
5.	Maximal proximal projection of greater trochanter.
6.	Gluteal tuberosity (lateralmost projection of the distal region of the greater trochanter)
7.	Distalmost point of lateral margin of trochanteric fossa.
8.	Medialmost projection of lesser trochanter
9.	Midpoint between landmarks 8 and 10
10.	Transition on medial edge between articular surface of femoral head and femoral neck

Table 1D. Landmark descriptions: tibia (*Martes pennanti* as representative species)

Landmark	Description
1.	Lateralmost projection of lateral epicondyle at the epiphysial line
2.	Lateralmost and proximalmost projection of the proximal edge of the lateral condyle
3.	Anterior intercondylar eminence
4.	Medialmost and proximalmost projection of the proximal edge of the medial condyle
5.	Medialmost projection of the medial epicondyle at the epiphysial line
6.	Medial edge of tibial tuberosity at epiphysial line
7.	Lateral edge of at tibial tuberosity at epiphysial line
8.	Midpoint of shaft on medial edge.
9.	Distalmost projection of medial malleolus.
10.	Proximalmost projection for flexor hallucis longus groove.
11.	Distalmost projection of the anterior edge of the distal articular surface
12.	Lateralmost projection of the distal edge of the fibular notch
13.	Midpoint of shaft on lateral edge.

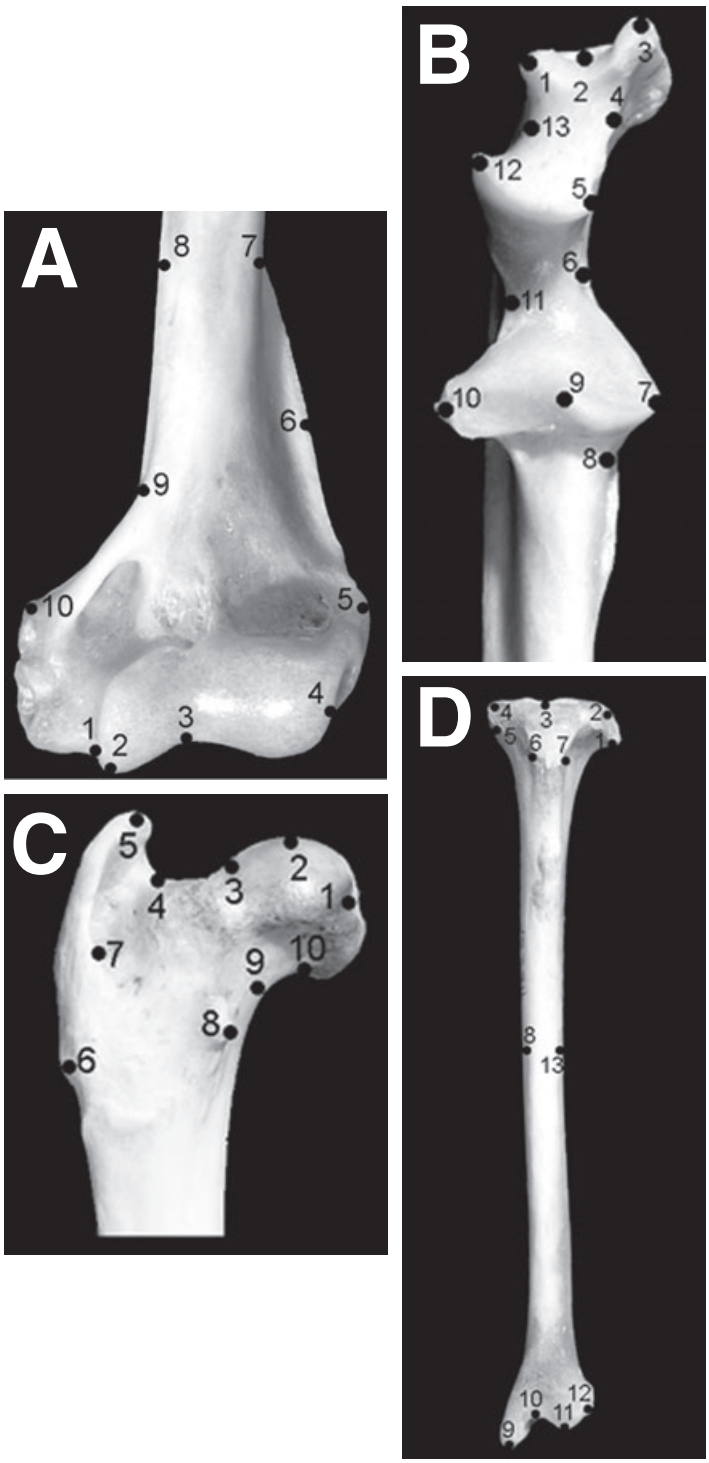

Figure 1. Landmark placement on four postcranial elements (*Martes pennanti* as representative species). A, humeral distal extremity. B, ulnar proximal extremity. C, femoral proximal extremity. D, complete tibia, cranial aspect.

mathematically as partial warps and the uniform component, respectively, and were generated using the tpsRelw software written by F. J. Rohlf 1998 (http://life.bio.sunysb.edu/morph/).

Locomotor categories

Compared with the locomotor diversity within the whole of the Carnivora, mustelids lack relatively high degrees of locomotor specialization (Simpson, 1945;

Holmes, 1980). This 'generalized' plan creates considerable difficulty when attempting to categorize mustelids because at first glance several genera can each fit into multiple categories. This tendency towards locomotor generalization underlines the importance of carefully defining each locomotor category. Several of the definitions used in this study are primarily based on Holmes (1980) and Taylor (1989), but often include modification or greater detail to create more accurate locomotor habit descriptions of these carnivores.

The half-bound locomotor mode is exemplified by members of the genus *Mustela*. An elongate body shape, shortened limbs relative to body length (Ewer, 1973; Czaplewski, Ryan & Vaughn, 1999) and similarity in the manner of prey capture (Ewer, 1973; Holmes, 1980) across all members of this genus produces a characteristically sinuous half-bound mode of locomotion (Gambaryan, 1974; Taylor, 1989). This locomotor mode is markedly different from that of other mustelid genera.

Fossoriality in musteloids is exemplified by badgers (represented in this study by *Taxidea taxus* and *Meles meles*) that use scratch digging rather their snouts or teeth for excavation (Hildebrand & Goslow, 2001). These two genera also produce extensive burrow systems and utilize excavation as a major mode of prey capture. As such, they spend a considerable amount of their active and rest time underground making them easy to classify as fossorial.

Scansorial locomotion is exemplified by swift-pursuit style arborealists that essentially run up trees and branches and do a great deal of jumping and leaping to capture prey. In particular, adaptations for this locomotor mode are most apparent when the substrate is less than horizontal and the animal must make adjustments to avoid slipping, or to descend trees without falling (Powell, 1981; Taylor, 1989). Often, members of this locomotor group possess semi-retractable claws (Powell, 1981; Clark *et al*., 1987; Pasitschniak-Arts & Lariviére, 1995) and the capacity to rotate the hind limb backward partially (Leach, 1977a, b) *Martes*, *Eira* and *Gulo* all fit this description well and are consequently classified in this study as scansorial.

Aquatic locomotion in mustelids is exemplified by the otters (represented in this study by *Lontra canadensis*, *Lutra lutra* and *Enhydra lutris*). Otters have developed specific gaits involving their hind limbs and tails, to propel them through water (Tarasoff *et al*., 1972). They also spend a large amount of time in the water; with *Enhydra* exhibiting reduced terrestrial locomotor abilities (Taylor, 1989).

The final locomotor category utilized in this study is ambulatory. Hildebrand & Goslow (2001) described the ambulatory gait as symmetrical with each foot being on the ground more than half the time. Thus, there is no floating phase. Many species use this gait exclusively (Taylor, 1989) because either their large size or aposematic colouring (along with a powerful scent) are their primary forms of predator avoidance. Both Holmes (1980) and Taylor (1989) classified skunks as ambulatory and their assessment is also used in this study with the inclusion of *Galictis* due to its similarity in gait to skunks.

We scored extant taxa using the five locomotor categories described above. Three of these categories followed Holmes (1980) directly. Of the two remaining categories, one is new reflecting the unique mode of locomotion exhibited by the genus *Mustela* (half-bound) and the other is a reclassification of Holmes's (1980) 'arboreal' category as scansorial in order to reflect more accurately that nature of this mode of locomotion. Table 2 summarizes the five locomotor categories and the taxa that fit into them.

Statistical analyses

To test whether the population means of the multiple dependent variables (the PW scores and the uniform component) are equal across locomotor groups, we first conducted a series of one-way multivariate analyses of variance (MANOVA). For each element, a MANOVA was conducted with locomotor mode as an independent variable with five categories: ambulatory, aquatic, scansorial, half-bound and fossorial. The dependent variables were the PW scores and the uniform component (shape measures).

The presence of a wide range of body sizes introduces the potential for an effect of size on shape differences across locomotor groups. Consequently, we wanted to perform a MANCOVA in order to test for shape differences across locomotor groups with centroid size as a covariate. Before completing a full MANCOVA analysis, however, we needed to perform a homogeneity-of-slopes test on each appendicular element data set (Zelditch *et al*., 2004). This test allowed us to determine if an interaction exists between centroid size and locomotor mode. If the homogeneity of slopes assumption was not violated and we could assume that the coefficients for centroid size were the same across locomotor modes, we could then perform a series of multivariate analyses of covariance (MANCOVA).

In order to assess how well individual element shapes differentiated between locomotor modes, we performed a canonical variates analysis (CVA) for all extant material of the unweighted partial warp scores matrix utilizing the CVAgen6n software package written by S. D. Sheets (http://www.canisius.edu/~sheets/morphsoft.html). By ordinating locomotor groups via CVA, we were able to use the CVA scores to determine which elements provide the greatest separation

Table 2. Locomotor category descriptions

Locomotor category	Description	Genera
Half-bound	Sinuous form of galloping. Suspended phase present.	*Mustela*
Fossorial	Scratch-digger, creates burrow systems, spends a large percentage of its time underground.	*Meles* *Taxidea*
Scansorial	Capable of swift pursuit of prey in trees; spend large percentage of time in trees.	*Eira* *Martes*
Aquatic	Specialized swimming gait, mostly utilizing the hind limb and caudal region the spine.	*Enhydra* *Lontra* *Lutra*
Ambulatory	Symmetrical, relatively slow gait with no floating phase.	*Galictis* *Gulo* *Mephitis* *Spilogale*

between functional categories relative to the separation between genera in the same category. We were also able subsequently to include fossil specimens into the sample as unknowns.

The CVAgen6 software determines the number of significant CVA axes at the 0.05 level that best discriminate between sets of known groups. The canonical variates scores of known specimens are then used to assign specimens to groups by utilizing the distance of that specimen from the mean of the nearest group (for a full discussion of this procedure see Nolte & Sheets, 2005). Assignments can then be cross-validated via a jackknifing procedure that leaves one known specimen out at a time, and then assigns it to a group using the data from the CVA axes for the remaining specimens. The number of repetitions used is determined by the number of specimens in the data set (http://www.canisius.edu/~sheets/morphsoft.html). In a separate procedure the CVA axes can then be used to assign unknown specimens) (Nolte & Sheets, 2005).

For this data set, we first ran a CVA for each element with the extant sample specimens assigned to the five locomotor groups described above. This first analysis allowed us to assess which locomotor groups were the most successfully reclassified over all, and which elements performed best at distinguishing between groups. We then ran a second analysis for each element, where we included the fossil *Trigonictis* samples as 'unknowns' in order to obtain locomotor mode predictions.

Finally, the CVAgen6 software allowed us graphically to present and describe the shape variation between and within locomotor modes. When plots of the canonical variates axes are generated using the CVAgen6 software shape representations can also be generated at any location in the morphospace. Thus, group centroid shapes can be represented as deformation plots away from the mean locomotor shape (e.g. Figs 2A–D, 3–6).

RESULTS

Multivariate analyses of shape variation

MANOVA analyses of the two shape measures (partial warp scores and uniform component) on the variable locomotor group indicated the existence of significant shape differences between locomotor groups ($P < 0.01$) (for a full summary of the MANOVA results see Table 3).

Results of the test of homogeneity of slopes between our covariate (centroid size) and our dependent variables (pw scores and uniform component) across all levels of locomotor mode showed a significant interaction in all four element data sets between locomotor mode and centroid size, suggesting that shape differences among locomotor modes varied as a function of size (Table 3).

Locomotor shape differentiation

The CVAs of locomotor modes produced four significant axes for each element with the first two axes producing the best separation between groups. Summary statistics for the four axes from each CVA analysis are provided in Table 4. We graphically presented locomotor modes by utilizing the canonical variates scores from the first two axes, and labelled specimens according to genus and locomotor mode. We then generated a series of deformations for each element from the con-

Table 3. Summary of MANOVA and homogeneity of slopes test results for all four elements with locomotor mode as the independent variable, PW scores and the uniform component and independent variables and centroid size as a covariate

Element	
	MANOVA summary statistics
Humerus	Wilk's $\lambda = 0.047$, $F_{72,962} = 15.746$, $P < 0.01$
Ulna	Wilk's $\lambda = 0.027$, $F_{88,912} = 15.393$, $P < 0.01$
Femur	Wilk's $\lambda = 0.045$, $F_{64,957} = 18.103$, $P < 0.01$
Tibia	Wilk's $\lambda = 0.031$, $F_{88,904} = 14.408$, $P < 0.01$
	Homogeneity of slopes summary statistics
Humerus	Wilk's $\lambda = 0.287$, $F_{72,942} = 4.882$, $P < 0.01$
Ulna	Wilk's $\lambda = 0.396$, $F_{88,892} = 2.679$, $P < 0.01$
Femur	Wilk's $\lambda = 0.42$, $F_{64,938} = 3.638$, $P < 0.01$
Tibia	Wilk's $\lambda = 0.252$, $F_{88,884} = 4.187$, $P < 0.01$

Table 4. Summary statistics for the four significant canonical variates axes identified for each specimen

Summary statistics	
Humerus CVA axes	
CV 1	Wilk's $\lambda = 0.0468$, $\chi^2 = 776.27$, d.f. = 72, $P < 0.01$
CV 2	Wilk's $\lambda = 0.1592$, $\chi^2 = 465.85$, d.f. = 51, $P < 0.01$
CV 3	Wilk's $\lambda = 0.3858$, $\chi^2 = 241.42$, d.f. = 32, $P < 0.01$
CV 4	Wilk's $\lambda = 0.7314$, $\chi^2 = 79.28$, d.f. = 15, $P < 0.01$
Ulna CVA axes	
CV 1	Wilk's $\lambda = 0.0273$, $\chi^2 = 869.40$, d.f. = 88, $P < 0.01$
CV 2	Wilk's $\lambda = 0.1043$, $\chi^2 = 545.99$, d.f. = 63, $P < 0.01$
CV 3	Wilk's $\lambda = 0.2949$, $\chi^2 = 294.93$, d.f. = 40, $P < 0.01$
CV 4	Wilk's $\lambda = 0.6459$, $\chi^2 = 105.56$, d.f. = 19, $P < 0.01$
Femur CVA axes	
CV 1	Wilk's $\lambda = 0.0448$, $\chi^2 = 783.89$, d.f. = 64, $P < 0.01$
CV 2	Wilk's $\lambda = 0.1505$, $\chi^2 = 478.21$, d.f. = 45, $P < 0.01$
CV 3	Wilk's $\lambda = 0.3614$, $\chi^2 = 257.00$, d.f. = 28, $P < 0.01$
CV 4	Wilk's $\lambda = 0.6484$, $\chi^2 = 109.39$, d.f. = 13, $P < 0.01$
Tibia CVA axes	
CV 1	Wilk's $\lambda = 0.0312$, $\chi^2 = 830.10$, d.f. = 88, $P < 0.01$
CV 2	Wilk's $\lambda = 0.1547$, $\chi^2 = 446.98$, d.f. = 63, $P < 0.01$
CV 3	Wilk's $\lambda = 0.3880$, $\chi^2 = 226.75$, d.f. = 40, $P < 0.01$
CV 4	Wilk's $\lambda = 0.7236$, $\chi^2 = 77.47$, d.f. = 19, $P < 0.01$

sensus to the centroid of each locomotor group. These deformations allowed us to illustrate and describe morphological differences between groups. Actual classification results are discussed in the next section.

The ambulatory locomotor group showed the poorest differentiation of any group in the CVA plots and possessed considerable spread throughout the plots (Fig. 2A–D). This group also showed the least differentiation from the consensus configuration in all elements (Figs 3–6). However, of the differentiation that was present, the ulna and femur showed the greatest amount and that corresponded with the best re-classification rates for the group The ulna showed the greatest deformation at the olecranon process with mild medial displacement of this feature ((landmarks 1–5 and 12–13). The femur showed slight lateral expansion of the greater trochanter at the gluteal tuberosity and trochanteric fossa (landmarks 6 and 7) but with little deformation anywhere else. The tibia and the humerus, in particular, differed little from the consensus configuration.

The aquatic functional group differentiated well in the CVA graphs of the humerus and tibia with overlap with other groups in the femur and ulna CVA graphs (Fig. 2A–D), although this overlap did not seem to affect re-classification rates in the femur (92%). The humerus showed expansion of the lateral epicondylar ridge at landmark 6 and compression of the lateral epicondyle at landmark 5. The medial epicondyle experienced the greatest deformation with medial expansion at landmark 10. The tibia had a broad and curved shaft (landmarks 8 and 13), medial displacement of the distal end (landmarks 9–12) and the proximal end was broadened medio-laterally (landmarks 1, 3 and 5–7). In the femur, the neck was short and broad (landmarks 3–4 and 9), whereas the greater trochanter was considerably expanded laterally (landmark 6). The femoral head was expanded distally at landmark 10 and lesser trochanter was also distally deviated (landmark 8). The ulna showed a lateral shift of the olecranon process at landmarks 1–5 and a medio-distal broadening of the olecranon at landmarks 5 and 12.

The fossorial functional group differentiated well in the CVA graphs of the ulna and tibia but showed considerable overlap with other locomotor groups in the humerus and femur (Fig. 2A–D). In the ulna the distal olecranon was lengthened and had strong lateral displacement of landmarks 1–5 and 13, producing pronounced medial curvature. The tibia displayed mild medial expansion near the medial condyle (landmark 5) along with a broadening of the shaft at landmark 8. The entire distal region (landmarks 9–12) shifted medio-distally and the flexor hallucis longus groove was relatively shallow and wide (landmarks 9–10). The humerus differed little from the consensus except for some lateral expansion of the epicondylar ridge at landmark 6 and some expansion of the medial epicondyle at landmark 10. The femur had a compressed gluteal tuberosity (landmark 6) and the lesser trochanter shifted medially (landmark 8). The femoral head shifted proximally and medially (landmarks 1 and 10) along with a shortening of the neck superiorly (landmark 4) and a lengthening of the neck inferiorly (landmark 9).

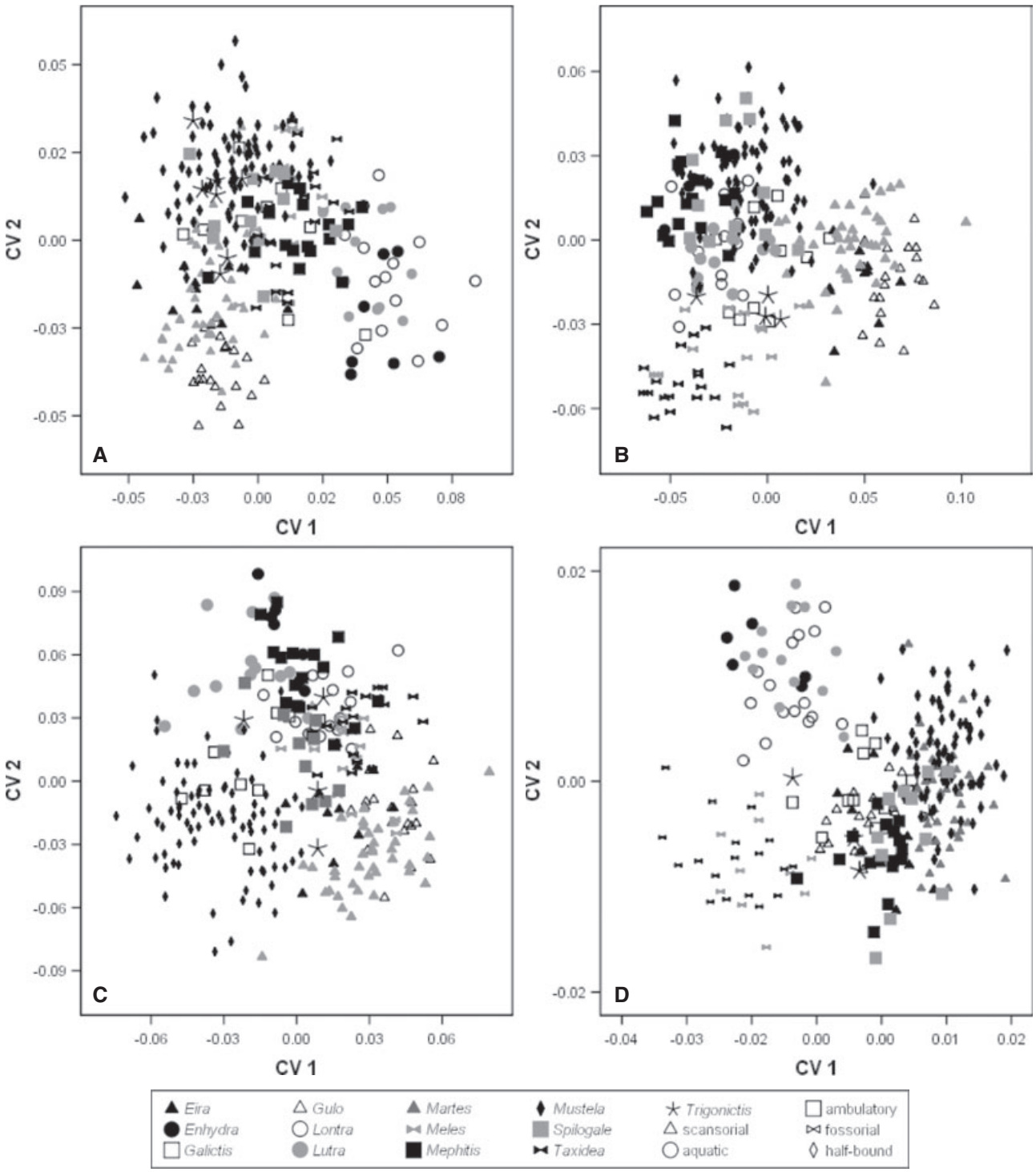

Figure 2. Canonical variates axes for CVA analyses on locomotor mode of extant and fossil mustelids. Symbol types represent locomotor modes and different colour symbols represent genera within locomotor modes. A, humerus. B, ulna. C, femur. D, tibia.

The half-bound locomotor category displayed some overlap with other functional groups on all the CVA graphs, particularly with the ambulatory group and with the scansorial group to a lesser extent (Fig. 2A–D). In the femur the greater trochanter was laterally expanded at the gluteal tuberosity (landmark 6) and the femoral head was expanded distally at landmarks 1 and 10. In the tibia all of the deformations from the

consensus were relatively small (Fig. 6). The shaft was slightly narrower and straighter. The flexor hallucis longus groove was deepened and narrowed (landmarks 9 and 10) and, overall, the distal and proximal ends were slightly narrowed. The ulna differed from the consensus shape with a medial shift of the olecranon at landmarks 1–5 and 12–13 that resulted in a narrowing and slight medial curvature as well as some shortening of the feature. Finally the humerus was slightly expanded at the lateral epicondyle (landmark 5) and at the lateral epicondylar crest (landmarks 6 and 7), but the medial epicondyle was constricted laterally (landmark 10).

The scansorial locomotor group showed differentiation from most groups in the CVA plots except for the tibia, where it overlapped with the ambulatory and half-bound groups. In the ulna the olecranon process was shortened and somewhat narrowed (landmarks 1–5 and 12–13) and the trochlear notch was slightly expanded distally (landmark 11). In the femur, the greater trochanter was constricted at landmarks 5 and 6 and the lesser trochanter was slightly shifted medially (landmark 8). The neck was lengthened and somewhat broadened (landmarks 4, 9 and 10) and the femoral head also shifted proximally (landmarks 1 and 10). The humerus experienced considerable deformation at the lateral epicondyle and lateral epicondylar ridge with a medial shift producing a relatively narrow distal humerus (landmarks 5–7). This narrowing is also evident to a lesser degree in the lateral shift of the medial epicondyle at landmark 10. The tibia exhibited deformation from the consensus configuration primarily at the distal end (landmarks 9–12) where there was a uniform lateral shift. The shaft was also slightly deviated laterally at landmarks 8 and 13.

Overall, three patterns emerged from the CVA analysis. First, functional groups displayed a gradient of morphological differentiation where more specialized groups (e.g. aquatic) were more often separated in shape space from other groups and coincided with the level of accuracy in re-classification for the group (Table 5). However, this separation occurred in some elements and not in others (e.g. the aquatic locomotor group's differentiation in the humerus and tibia CV axes, but not in the ulna and femur axes). Conversely, more generalized locomotor groups (e.g. ambulatory and half-bound) consistently overlapped with other groups. Second, within some locomotor categories, shape differences between genera were also present (e.g. *Martes*, *Eira* and *Gulo* within scansorial) and indicated that shape differences in postcranial elements may also be used to generate genus classifications, particularly in the

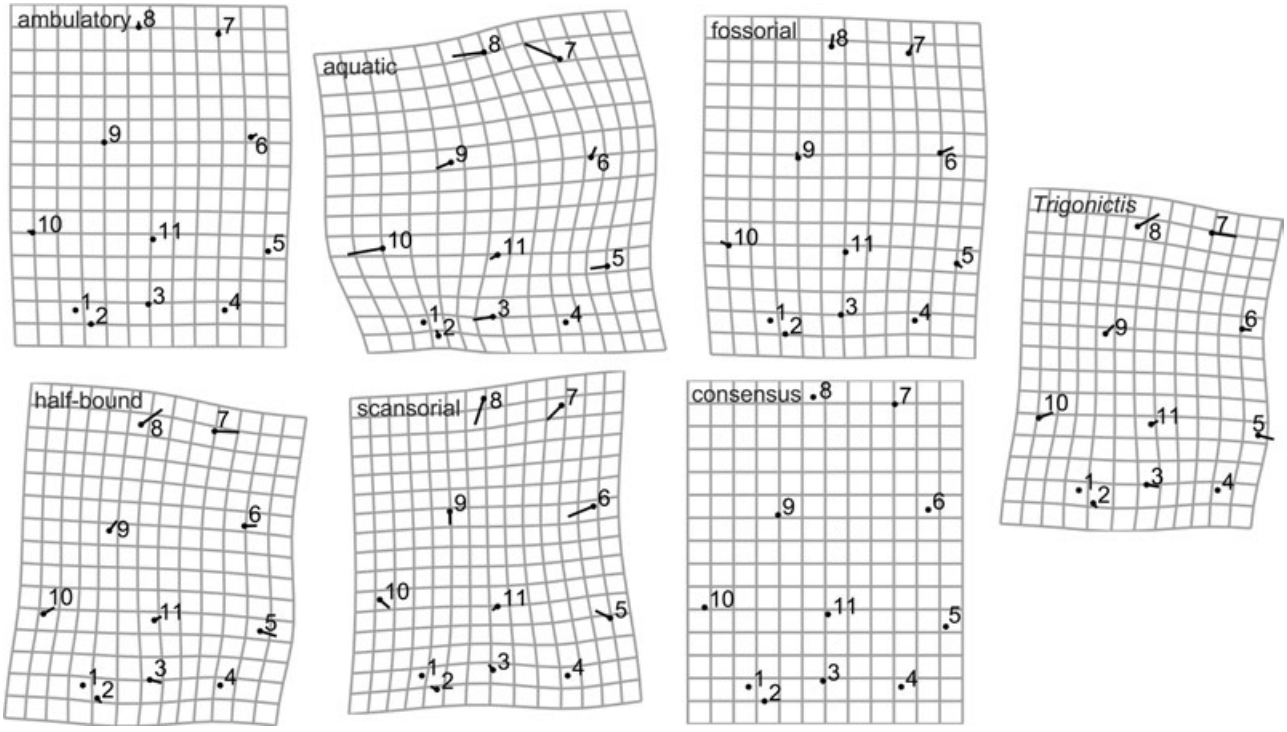

Figure 3. Humeral element deformations from the consensus configuration produced by the CVA analysis for locomotor mode; each deformation represents the shape corresponding to the mean CVA score for a particular locomotor group.

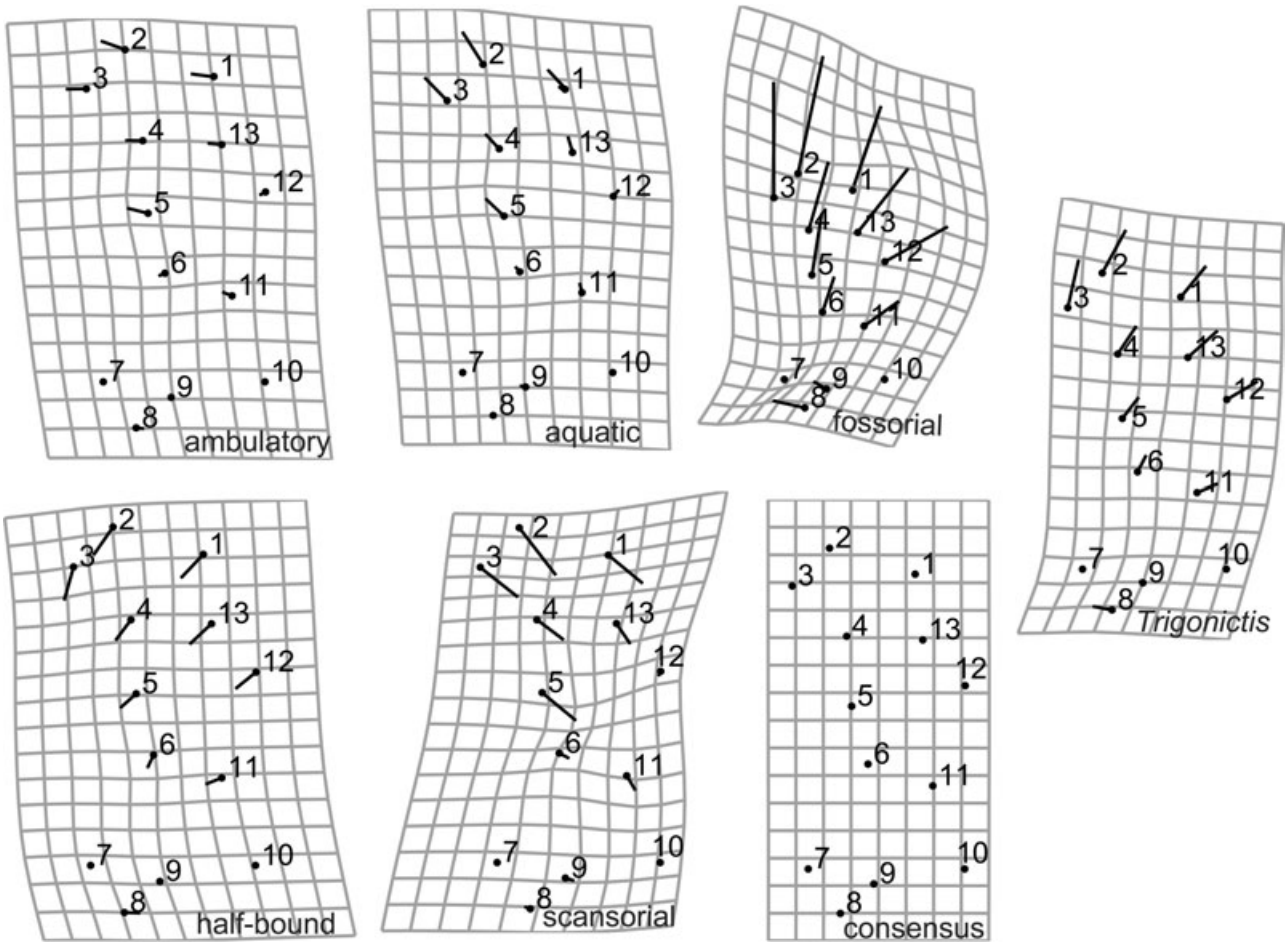

Figure 4. Ulnar element deformations from the consensus configuration produced by the CVA analysis for locomotor mode; each deformation represents the shape corresponding to the mean CVA score for a particular locomotor group.

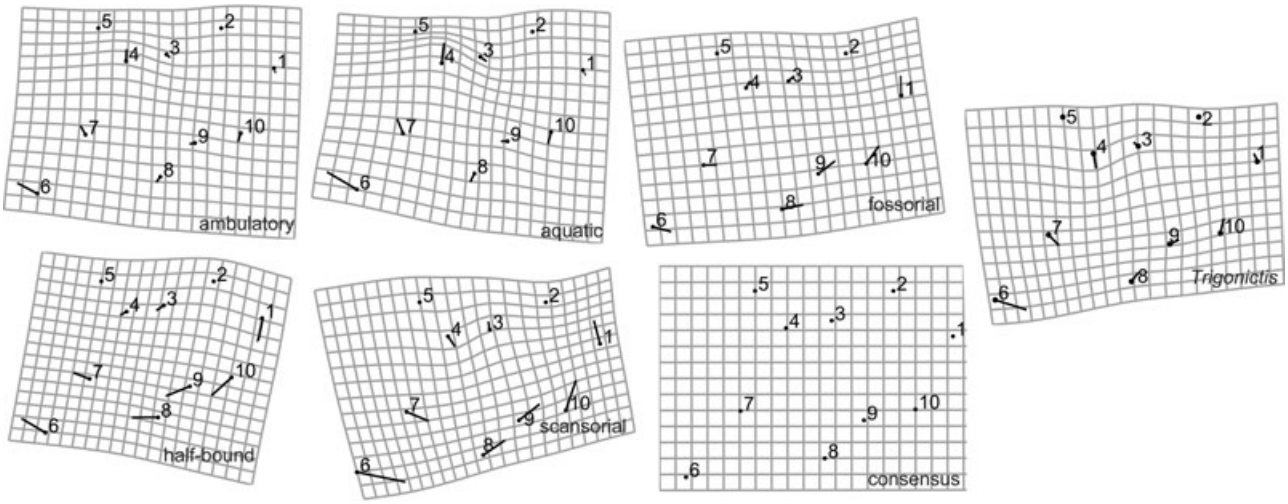

Figure 5. Femoral element deformations from the consensus configuration produced by the CVA analysis for locomotor mode; each deformation represents the shape corresponding to the mean CVA score for a particular locomotor group.

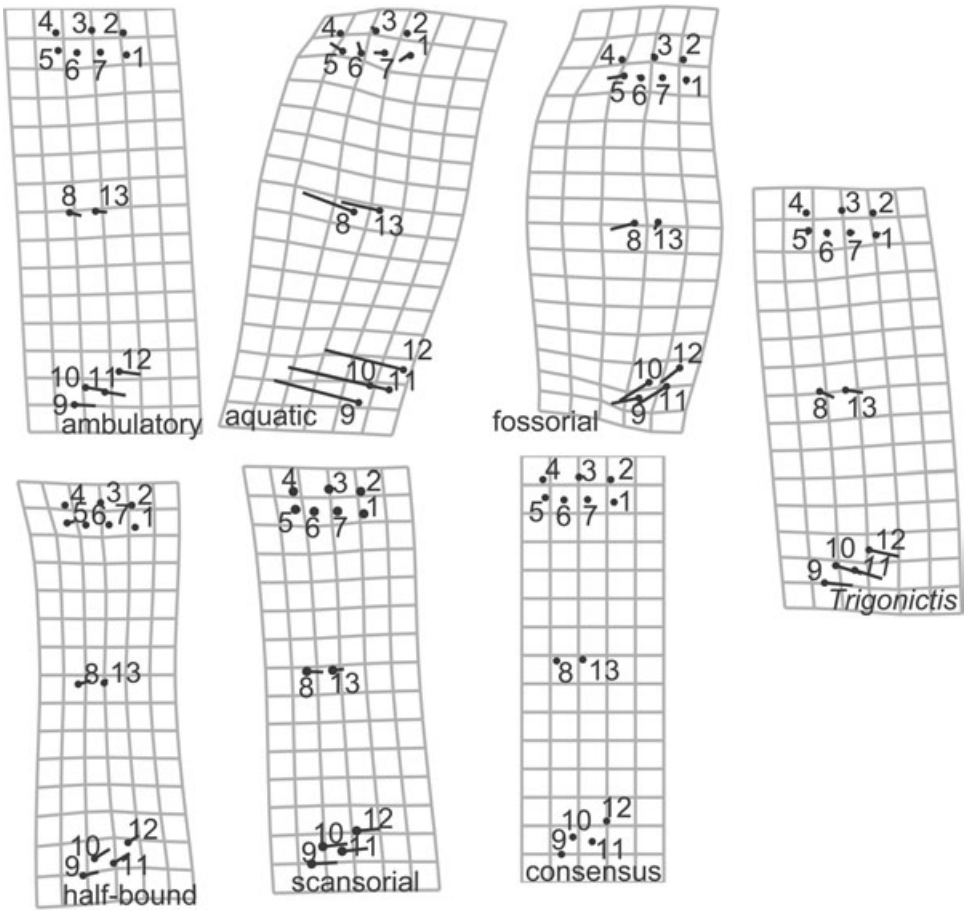

Figure 6. Tibia element deformations from the consensus configuration produced by the CVA analysis for locomotor mode; each deformation represents the shape corresponding to the mean CVA score for a particular locomotor group.

more specialized locomotor groups. Third, the lack of a consistent degree of differentiation between locomotor groups on all of the CVA axes along with the re-classification results (discussed below) suggested a tendency towards shared morphological characteristics between some groups.

Locomotor mode predictions

Extant taxa

For the CVAs, the jacknifed percentage of correct classifications for locomotor mode was relatively high across elements (Table 5). However, variability existed in levels of accurate reclassification when the within-element results were examined. Across all locomotor modes, the highest percentage of correct classification was achieved when using the shape data on the femur (84.1%) and ulna (83.9%), but overall reclassification results for all elements were comparable (humerus 77.8%, tibia 77.6%). In addition, certain locomotor modes were correctly classified more often than others. The average reclassification accuracy for each group was as follows (from greatest to least): fossorial 89.3%. aquatic 89%, scansorial 84.3%, half-bound 80.3%, ambulatory 61.5%.

Finally, when we examined the reclassification accuracy for locomotor modes across elements, we found that accuracy varied considerably such that certain elements were much more successful at classifying certain locomotor types than others. For example, for scansorial locomotion, the ulna performed better in the re-classification procedure (96%) than did the remaining elements (femur 86%, humerus 84%, tibia 71%). By contrast for fossorial locomotion, the tibia performed better in the re-classification procedure (96%) that did the remaining elements (ulna 94%, femur 84%, humerus 83%). Table 5 presents the reclassification matrices for each element. These results suggest that the shape of all elements can be used for locomotor mode classification, but that certain elements predict certain locomotor functions better than others.

Table 5. Jacknifed (with one known specimen left out at a time and assigned using the CVA axes) re-classification matrices for each element. The average re-classification success for each group was: fossorial 89.3%, aquatic 89%, scansorial 84.3%, half-bound 80.3%, ambulatory 61.5%

	Scansorial	Aquatic	Ambulatory	Fossorial	Half-bound
Humerus, 77.82% overall					
Scansorial (n = 74)	**66**	0	3	0	9
Aquatic (n = 34)	0	**31**	2	1	0
Ambulatory (n = 39)	4	1	**23**	6	5
Fossorial (n = 35)	1	0	3	**29**	2
Half-bound (n = 84)	8	2	6	6	**62**
Ulna, 83.98% overall					
Scansorial (n = 72)	**69**	1	0	0	2
Aquatic (n = 33)	0	**27**	5	0	1
Ambulatory (n = 38)	3	1	**25**	4	5
Fossorial (n = 34)	1	0	1	**32**	0
Half-bound (n = 79)	3	3	9	2	**62**
Femur, 84.09% overall					
Scansorial (n = 73)	**63**	1	1	7	1
Aquatic (n = 36)	1	**33**	1	0	1
Ambulatory (n = 38)	0	4	**26**	1	7
Fossorial (n = 32)	2	2	1	**27**	0
Half-bound (n = 85)	4	1	5	2	**73**
Ulna, 77.56% overall					
Scansorial (n = 72)	**51**	0	12	0	9
Aquatic (n = 35)	1	**32**	1	1	0
Ambulatory (n = 38)	11	2	**20**	1	4
Fossorial (n = 28)	0	0	1	**27**	0
Half-bound (n = 81)	8	0	6	0	**67**

Locomotor mode of Trigonictis

The CVAs also generated classifications of locomotor mode for the fossil sample. Table 6 shows the classifications generated by the CVA for each of the four fossil element samples.

The first sample contained all of the extant humeri used in the original analysis and seven fossil humeri. Six of the fossils represented *Trigonictis macrodon* and one represented *Trigonictis cookii* (Table 6). The locomotor classifications for the humeral *Trigonictis* fossil sample were five half-bound and two scansorial.

The second sample contained all of the extant ulnae used in the original analysis and three fossil ulnae. All of the fossils represented *Trigonictis cookii* (Table 6). The locomotor classifications for the fossil *Trigonictis* sample were fossorial, scansorial and aquatic.

The third sample contained all of the extant femora used in the original analysis and four fossil femora. Three of the fossils represented *Trigonictis macrodon* and one represented *Trigonictis cookii* (Table 6). The locomotor classifications for the femoral *Trigonictis* sample were aquatic, scansorial and half-bound.

The fourth sample contained all of the extant tibiae used in the original analysis and four fossil tibiae. Two of the fossils represented *Trigonictis macrodon*, one represented *Trigonictis cookii* and one represented *Trigonictis* sp. The locomotor classifications for the tibial *Trigonictis* sample were one ambulatory, two scansorial and one fossorial.

Overall, the CVAs produced locomotor mode classifications for the fossil *Trigonictis* elements that may be described as follows: the two most prominent predictions were half-bound (six of 16 specimens) and scansorial (six of 16 specimens). These were followed by fossorial (two of 16), aquatic (two of 16) and ambulatory (one of 16 specimens).

The exceptional University of Michigan specimen (UMMP 49819) provided us with all four of the elements used in this study in a single individual. Consequently, predictive results for elements from this specimen are worth examining in isolation. The CVA results for this individual classified one element as half-bound with the remaining three elements classified as scansorial.

Table 6. CVA-generated predictions for locomotor mode in the fossil femora. We list the specimen numbers and original identifications, our qualitative identifications (author ID), and the predictions of the CVA analysis per element. Note that blank spaces indicate that a given element was not available for this specimen. The specimen in bold type is a nearly complete skeleton of *Trigonictis cookii* with all four elements used in this study present

Specimen no.	Author ID	humerus	Ulna	Femur	tibia
Unidentified (USNM 2021416)	*Trigonictis macrodon*	scansorial	fossorial		
***Trigonictis cookii* (UM 49819)**	***Trigonictis cookii***	**½ bound**	**scansorial**	**scansorial**	**scansorial**
Trigonictis macrodon (UM 53554)	*Trigonictis macrodon*	scansorial			
Trigonictis macrodon (UM 53556)	*Trigonictis macrodon*	½ bound			
Trigonictis macrodon (UM 55001)	*Trigonictis macrodon*	½ bound			
Trigonictis macrodon (UM 51376)	*Trigonictis macrodon*	½ bound			
Trigonictis macrodon (UM 51049)	*Trigonictis macrodon*	½ bound			
Trigonictis cookii (IMNH 1100)	*Trigonictis cookii*		aquatic		
Trigonictis cookii (IMNH 571)	*Trigonictis cookii*		fossorial		
Trigonictis macrodon (UM 54683)	*Trigonictis macrodon*			scansorial	
Trigonictis macrodon (UF 14256)	*Trigonictis macrodon*			aquatic	
Trigonictis macrodon (UF 16762)	*Trigonictis macrodon*			half-bound	
Trigonictis sp. (HAFO 387)	*Martes*				scansorial
Trigonictis macrodon (UM 56096)	*Trigonictis macrodon*				fossorial
Trigonictis macrodon (UF 18475)	*Trigonictis macrodon*				ambulatory

Latent effects of size

Because the homogeneity of slopes test demonstrated that a significant interaction between locomotor mode and centroid size exists, we wanted to evaluate whether the observed differentiation along the CV axes was influenced by size. To do so, CVA scores were regressed on size for each element data set. The linear regressions for all significant axes within the four elements demonstrate that the regression coefficients were with one exception relatively low. These results in conjunction with the considerable data spread (as illustrated by the bivariate plots in Fig. 7) indicate poor prediction of CV score by centroid size. Humerus: (CV1 vs. size $r^2 = 0.009$; CV2 vs. size $r^2 = 0.032$; CV3 vs. size $r^2 = 0.0006$; CV4 vs. size $r^2 = 0.002$). Ulna: (CV1 vs. size $r^2 = 0.005$; CV2 vs. size $r^2 = 0.451$; CV3 vs. size $r^2 = 0.077$; CV4 vs. size $r^2 = 0.001$). Femur: (CV1 vs. size $r^2 = 0.001$; CV2 vs. size $r^2 = 0.090$; CV3 vs. size $r^2 = 0.009$; CV4 vs. size $r^2 = 0.002$). Tibia: (CV1 vs. size $r^2 = 0.230$; CV2 vs. size $r^2 = 0.004$; CV3 vs. size $r^2 = 0.196$; CV4 vs. size $r^2 = 0.038$).

As mentioned above, the one exception found in the regression results was in the relationship between centroid size and CV2 scores of the ulna. Given that 45% of the variance explained by CV2 in the ulna is related to size, and the spread around the regression line is minimal (Fig. 7B), we can reasonably assume that for this particular axis, size plays a large role in ulnar shape differentiation.

DISCUSSION

Locomotor shape differences and size

In our analyses of locomotor mode, we not only showed significant shape differences between locomotor groups, but also demonstrated that an interaction between shape, size and locomotor function exists. When we tested for the magnitude of this interaction with regard to shape differentiation along CV axes, we found little effect, except in CV2 of the ulna. In this particular axis, the ulna exhibited an almost linear trend in shape change that coincided with low scores along CV2 and centroid size increased. This trend appears to be driven by the fossorial functional group, which represents some of the larger specimens in the sample and showed a broadening of the olecranon process in the medio-lateral plane (Figs 2B, 4) negatively along CV2.

Allometry of appendicular elements in mammals is well recognized, and changes in length, robusticity and overall limb orientation are thought to result from adaptations to the mechanical loads produced by increased body size (Biewener, 1989). In a study focused on mustelids, Heinrich & Biknevicius (1998) found allometric effects in long bone length and linear measures of robusticity relative to body size such that load-bearing regions of skeletal elements react positively in response to increases in size. Additionally, they demonstrated that these patterns differ between

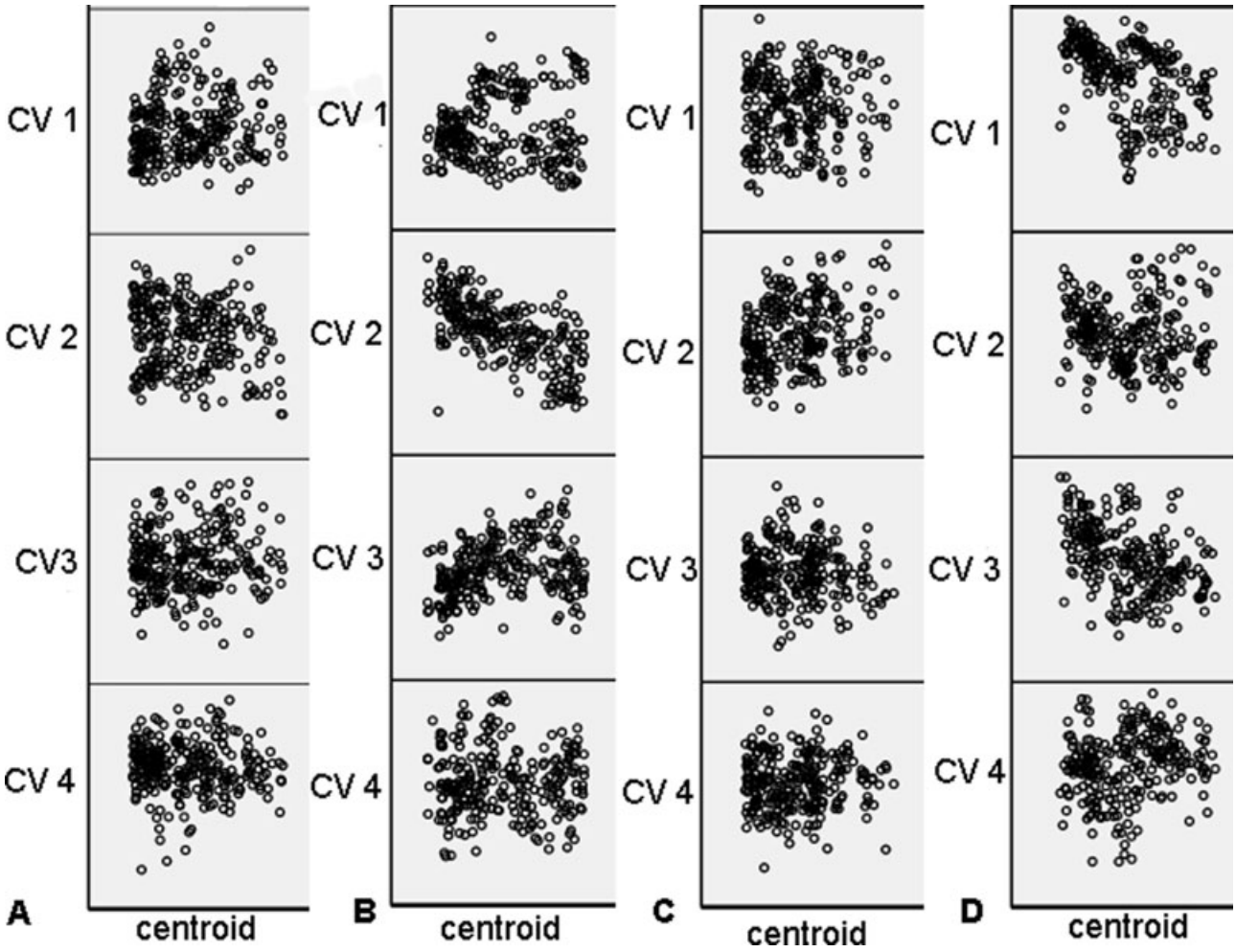

Figure 7. Plots of centroid size and canonical variates scores for each element. A, humerus. B, ulna. C, femur. D, tibia.

lineages with different locomotor modes; these differing patterns indicate that locomotor function either plays a role in or is affected by this allometric relationship. Given that certain locomotor behaviours generate greater mechanical stressors than others (Christiansen, 1999), our findings, especially for the ulna, moderately support a possible allometric relationship between shape of appendicular elements and locomotor mode in a larger sample of mustelids. However, because we did not directly test for an allometric relationship, they are not definitive.

Functional implications

Ambulatory

In all cases, the elements of ambulatory mustelids closely resembled the consensus configuration and this was most apparent in the humerus (Fig. 5) where deformation is nearly non-existent. Ambulatory mustelids also repeatedly overlapped with other groups on the CVA axes. This result was consistent with the observations of van de Graaff, Harper & Goslow (1982) and Taylor (1989) who categorized ambulatory carnivores as ancestral and unspecialized.

Aquatic

Aquatic mustelids were well differentiated along the CV1 and CV2 axes in the humerus and tibia with less differentiation in the femur and ulna. However, unlike in other groups, the level of morphological differentiation along these axes did not correspond to the level of re-classification success entirely.

The humerus had both good differentiation along the CV1 and CV2 axes (Fig. 2A) and good re-classification rates (91%, Table 5) and an expanded lateral epicondylar ridge and an expanded medial epicondyle. These structures serve as the sites of origin for various muscles that flex, pronate and supinate the forearm and flex and extend the wrist. Thus, although rapid

propulsion during aquatic locomotion is generated by the hind limb, a great deal of fore-limb motion also occurs, focused primarily in the forearm (Maynard Smith & Savage, 1956; Tarasoff *et al*., 1972; Taylor, 1989; Fish, 1994).

The tibia of aquatic mustelids also differentiated well (Fig. 2D) and had a re-classification rate of 91% (Table 5). It had a distinctively curved shaft and a broadened flexor hallucis longus groove caused in part by the shortening of the medial malleolus. The flexor hallucis longus groove is a region of passage for the tendons of posterior muscles of the leg involved in dorsiflexion, inversion and plantar flexion. Because much of the propulsive force during aquatic mustelid locomotion is generated at the rear limb via dorsiflexion and plantar flexion (Tarasoff *et al*., 1972; Tarasoff, 1972), these shape deformations of the tibia were not unexpected.

The femur differentiated poorly along the CV1 and CV2 axes (Fig. 2C) but had a very good re-classification rate of 92% (Table 5). There was a tendency for the femur to be short and robust, particularly at the greater trochanter and gluteal tuberosity. These are attachment sites for the gluteal muscles that extend and abduct the hip and produce much of the propulsive power while swimming.

Finally, the ulna, which displayed poor differentiation along the CVA axes (but still had relatively good re-classification results at 82%, Table 5), had some elongation and broadening of the olecranon and was somewhat similar in shape to the ambulatory ulna (Fig. 4).

Fossorial

Both *Meles* and *Taxidea* are scratch diggers (Taylor, 1989; Hildebrand & Goslow, 2001). Subsequently, most of the effort and force of excavation is generated by adduction and abduction of the forelimb and is focused on the claws that must break up hardened soil (Wagner, 1976). The hindlimb is used primarily in kicking the loosened soil out of the burrow (Shimer, 1903; Taylor, 1989; Nowak, 2000). Because the forelimb plays a primary role in excavation leading to hypertrophy of the upper limb musculature (Shimer, 1903; Wagner, 1976) its elements were expected to exhibit the greatest level of deformation from the mean form relative to the elements of the hind limb. However, this expectation was not entirely borne out by the results; rather it was the distal elements of the front and hind limbs that demonstrated the greatest levels of deformation and the proximal elements showed the least.

The tibia had good separation on the CV1 and CV2 axes (Fig. 2D) and a re-classification rate of 96% (Table 5). The tibia had a broad and slightly curved shaft as well as a medial shift of the distal articular region and a shallow and broad flexor hallucis longus groove. As in aquatic mustelids, dorsiflexion, plantar flexion and overall rotation of the pes are critical motions. Consequently, the flexor hallucis longus, flexor digitorum longus and tibialis posterior all require a large insertion site at the tibial shaft and ample room for passage of the tendons at the flexor hallucis longus groove. However, instead of propelling the animal, the aforementioned movements mobilize soil from the burrow after initial excavation. Therefore, although the two locomotor groups utilize similar motions and muscle groups producing some similar trends in deformation, their tibial shapes differ as the forces generated are different and the amount of rotation of the pes is also likely to be different. This difference is illustrated by the fact that the fossorial and aquatic tibiae both lie in the same region of the CV1 axis (Fig. 2D) but differentiate along the CV2 axis.

The ulna not only separated well on the CV1 and CV2 axes (Fig. 2B), but also showed separation between fossorial genera and had a re-classification rate of 94% (Table 5). As expected, the ulna was robust and strongly differentiated with a long and curved olecranon, a site of attachment for wrist flexors and forearm extensors. The lengthening of this feature generates greater power to the claws, which experience great stress during scratch digging (Maynard Smith & Savage, 1956; Quaife, 1978; Van Valkenburgh, 1985; Taylor, 1989). Maynard Smith & Savage (1956) found that the olecranon is elongated in both fossorial and aquatic mammals. However, our results demonstrate that although the relative length of the olecranon is increased for both modes of locomotion, shape aspects, particularly the curvature of the olecranon (Fig. 4), differentiate between the two groups.

Both the femur and the humerus were robust and are clearly active during digging, but they did not differentiate as well (nor produce the same level of classification results, 84% and 83%, respectively) as the ulna and tibia. The shapes of these two elements often overlapped with those of ambulatory mustelids (Fig. 2A, B).

The femur had a slightly shortened neck and lateral expansion of the gluteal tuberosity along with a medial shift of the lesser trochanter. The gluteal tuberosity serves as the insertion site for the gluteus maximus, a powerful thigh extensor. The lesser trochanter is the insertion site for the iliopsoas, a flexor of the hip and a lateral flexor of the vertebral column. All of these muscles are most active when movement occurs from a static pelvic position, which occurs during excavation as the soil that is generated by the action of the forelimb is pushed backward from the burrow by the hindlimb (Shimer, 1903).

The humerus showed the least level of deformation from the consensus configuration, a result that was unexpected given discussion in the literature regarding humeral morphology in fossorial mammals (Shimer, 1903; Wagner, 1976). The large contribution of the humerus to excavation created the expectation that this element in fossorial mustelids would differentiate strongly from humeri of other locomotor groups. However, this was not the case and we suspect that this was caused by the relatively robust nature of the mean humeral form, such that only extremely robust humeri (like those of aquatic mustelids) or extremely gracile ones (those of scansorial mustelids) differed significantly from the consensus configuration.

Half-bound

The half-bound mode of locomotion is most efficient for small, unspecialized mammals traversing a variable landscape (Hildebrand, 1977; Taylor, 1989). In mustelids, this form of locomotion tended to produce element shapes that clustered near other groups (particularly ambulatory and scansorial) except for the femur, which showed not only the best differentiation along the CV1 and CV2 axes (Fig. 2C) but also had the best reclassification rate (86%, Table 5).

The femur had an expanded gluteal tuberosity and a relatively enlarged and rounded femoral head. The half-bound has two alternating phases of spinal flexion and extension requiring that full support of body weight alternate between the front and hind limbs (Gambaryan, 1974). In particular, during spinal extension, the propulsive thrust for the half-bound is generated by the hind limbs whereas the forepaws serve primarily as a break (Williams, 1983). The gluteus maximus inserts at the gluteal tuberosity of the femur and is a major extensor of the thigh and would be the main actor during spinal extension.

The tibia, although overlapping considerably with that of scansorial mustelids on the CV1 and CV2 axes (Fig. 2D), had a re-classification rate of 86% (Table 5) and was relatively gracile and straight with narrowed distal and proximal ends and a deep and narrow flexor hallucis longus groove. The deepening of the groove is created by the distal extension of the medial malleolus, which may provide mediolateral stability of the tibio-astragalus joint. This joint would receive considerable stress during the initiation of the bound as all of the animal's weight is supported by the foot during plantar flexion.

The remaining two elements overlapped considerably with other groups and their re-classification rates (ulna 78%, humerus 74%) and rates of incorrect classification (Table 5) reflect this overlap in morphology.

Scansorial

Three elements in particular showed morphological differences from the consensus, the ulna, humerus and femur. The ulna had the best separation along the CV1 and CV2 axes (Fig. 2B) along with the best re-classification rate for the group at 96% (Table 5). The morphology of the scansorial ulna is quite distinct due to its shortened olecranon. This olecranon provides an enlarged insertion site for the triceps brachii, the primary extensor of the forearm. Scansorial climbing involves use of the forearm to create propulsion up trees, with the forearm extensors generating considerable power and consequently requiring strong attachment sites (Taylor, 1974, 1989).

The femur of scansorial mustelids also separated well along the CV1 and CV2 axes with minor overlap with the fossorial group (Fig. 2C) and had a re-classification rate of 86% (Table 5). The femur had marked expansion of the lesser trochanter. This expansion indicated a greater use of hip rotators during locomotion, assumed to be associated with increased climbing ability (Taylor, 1976).

The humerus of scansorial mustelids generally separated well along the CV1 and CV2 axes, but had some overlap with the ambulatory and half-bound groups (Fig. 2A) and had a re-classification rate of 84% (Table 5). The humerus was distinct in the reduction of the lateral epicondyle and the lateral epicondylar ridge, as well as some overall lengthening. As discussed above most of the propulsive force in scansorial climbing is generated by the forearm extensors (triceps brachii), which originate at the scapula and on the proximal end of the shaft and insert on the olecranon process of the ulna. This type of locomotion requires considerable stability at the elbow joint and is characterized by a hinge-like morphology that constricts medio-lateral movement (Andersson, 2004). Within mustelids, it appears that this constriction is also accompanied by some reduction of the wrist and finger extensors and the abductors and supinators of the wrist (anconeus and supinator) that originate at the lateral epicondyle and lateral supracondylar ridge.

The tibia was little changed from the consensus configuration in scansorial mustelids and overlaps considerably with the ambulatory and, in particular, the half-bound locomotor groups along the CV1 and CV2 axes (Fig. 2D). This element also had a considerable reduction in re-classification accuracy (71%, Table 5) relative to the other three elements.

Locomotor mode predictions

Extant taxa

The high frequency of correct re-classification for all elements examined demonstrated that dense articular regions of any long bone may be used to produce loco-

motor predictions in mustelid carnivores. However, predictions may be most reliable when multiple elements are used and when more specialized rather than more generalized groups are examined. Additionally, shape descriptors displayed the potential for distinguishing between those taxonomic groups that shared similar locomotor adaptations. Thus, differentiation of appendicular elements was possible at the genus level, but again may be most effective for groups exhibiting functional specialization.

Trigonictis

Our goal was to utilize the distance-based method of Nolte & Sheets (2005) to assign a set of unknown fossils to known locomotor groups utilizing two-dimensional morphometric data.

The results of these assignments indicated that the two species of *Trigonictis* possessed a locomotor pattern that was most probably half-bound or scansorial. However, our results also show locomotor predictions for *Trigonictis* that are spread throughout the range of locomotor modes in lower frequencies. Three possible explanations exist for this disparity in assignment.

First, we believe that the interaction between size and shape, although moderate, was an important factor in the emergence of musteloid functional specialization such that locomotor diversity and specialization in musteloids occurred in conjunction with shifts in body size. Thus, it seems likely that taxa on the more unspecialized end of the spectrum, which were also smaller, possessed a common morphological 'toolkit' that may have allowed them to assume various functional roles with shifts in body size. The size of *Trigonictis* lay between that of half-bound musteloids and scansorial and ambulatory musteloids and, as might be expected, *Trigonictis* element shapes were also intermediate between these groups (particularly scansorial and half-bound), perhaps driven by these size relationships.

Second, our findings show that assignment accuracy is elevated for more specialized, rather than more generalized groups and that *Trigonictis* specimens generally ordinate in the more generalized shape space. Thus, the generalized nature of *Trigonictis* appendicular elements probably explains why previous assessments have gone back and forth between genera representing the more generalized locomotor modes.

Finally, it is important to remember that *Trigonictis* is an extinct genus that may have had a distinctive mode of locomotion intermediate between the half-bound and scansorial locomotor categories. This possibility, considered alongside our findings that reassignment success varied depending on which element and which locomotor mode was being examined, suggests that within mustelid carnivores, locomotor specialization originates from a relatively generalized form and does not require the modification of all skeletal elements, only those most impacted by a locomotor shift.

Although this analysis is not completely conclusive regarding the locomotor mode of *Trigonictis*, the power of the method to limit the choices is clear. We have demonstrated that locomotion in *Trigonictis* was probably generalized and closest to those of half-bounding (e.g. *Mustela*) and scansorial (e.g. *Martes*) mustelids. The overall accuracy of the CVA analyses utilizing shape data is encouraging for future use of the technique on additional fossil taxa. We have developed a database of postcranial element shape that is particularly suited to the examination of fossil specimens. Our results show that appendicular element shape data, even data on only a portion of the complete element, produce robust identification results. Future researchers may be able to utilize this database to extract information from fossil fragments at a greater level of resolution than before.

ACKNOWLEDGEMENTS

We would like to thank the following institutions for permission to study both extant and fossil material: University of Colorado Museum of Natural History (UCM), Denver Museum of Nature and Science (DMNS), the Museum of Southwestern Biology (MSB), National Museum of Natural History (NMNH), Idaho Museum of Natural History (IMNH), Natural History Museum of Los Angeles County (LACM), Hagerman Fossil Beds National Monument (HAFO), University of Michigan Museum of Paleontology (UMMP), the Florida Museum of Natural History (UFL), the Swedish Museum of Natural History (NRM), the Natural History Museum, London (NHM), the National Museum of Scotland (NMS) and the Field Museum in Chicago. We would also like to thank D. M. Armstrong, M. Krest and J. Krieger for their valuable feedback during the preparation of this paper. B. VanValkenburgh and P. D. Polly provided critical reviews of a previous version of this work that significantly improved the quality of this paper. Additionally, we would like to acknowledge the critical initial input of G. McDonald, without whom this work would never have originated. This study was made possible through financial support from the University of Colorado Graduate School and the University of Colorado Museum.

REFERENCES

Anderson E. 1989. The phylogeny of mustelids and the systematics of ferrets. In: Thorne ET, Bogan M, Anderson SH, eds. *Conservation biology of the blackfooted ferret*. Connecticut: Yale University Press, 10–20.

Andersson K. 2004. Elbow–joint morphology as a guide to forearm function and foraging behavior in mammalian carnivores. *Zoological Journal of the Linnean Society* **142:** 91–104.

Biewener AA. 1989. Mammalian terrestrial locomotion and size. Mechanical design principles define limits. *Biosciences* **39:** 776–783.

Bininda-Emonds ORP, Gittleman JL, Purvis A. 1999. Building large trees by combining phylogenetic information: a complete phylogeny of the extant Carnivora (Mammalia). *Biological Review* **74:** 143–175.

Bjork PR. 1970. The Carnivora of the Hagerman local fauna (late Pliocene) of southwestern Idaho. *Transactions of the American Philosophical Society* **60:** 1–54.

Bonnan MF. 2004. Morphometric analysis of humerus and femur shape in Morrison sauropods: implications for functional morphology and paleobiology. *Paleobiology.* **30:** 444–470.

Bookstein FL. 1991. *Morphometric tools for landmark data: geometry and biology*. London: Cambridge University Press.

Bryant HN, Russel AP, Fitch WD. 1993. Phylogenetic relationships within the extant Mustelidae (Carnivora): appraisal of the cladistic status of the Simpsonian subfamilies. *Zoological Journal of the Linnean Society* **108:** 301–334.

Christiansen P. 1999. Scaling of the limb long bones to body mass in terrestrial mammals. *Journal of Morphology* **239:** 167–190.

Clark TW, Anderson E, Douglas C, Strickland M. 1987. *Martes americana*. *Mammalian Species* **289:** 1–8.

Czaplewski N, Ryan JM, Vaughn TA. 1999. *Mammalogy*, 4th edn. Texas: Saunders Press.

Dragoo JW, Honeycutt RL. 1997. Systematics of mustelid-like carnivores. *Journal of Mammalogy* **78:** 426–443.

Ewer RF. 1973. *The carnivores*. London: Weidenfield and Nicholson.

Fish FE. 1994. Association of propulsive swimming mode with behavior in river otters (*Lutra canadensis*). *Journal of Mammalogy* **55:** 989–997.

Flynn JJ, Neadbal MA, Dragoo JW, Honeycutt RL. 2000. Whence the red panda? *Molecular Phylogenetics and Evolution* **17:** 190–199.

Gambaryan PP. 1974. *How mammals run. Anatomical adaptations.* New York: John Wiley and Sons.

Gazin CL. 1934. Upper Pliocene mustelids from the Snake River Basin of. Idaho. *Journal of Mammalogy* **15:** 137–149.

van de Graaff KM, Harper J, Goslow GE Jr. 1982. Analysis of posture and gait selection during locomotion in the striped skunk (*Mephitis mephitis*). *Journal of Mammalogy* **63:** 582–590.

Heinrich RE, Biknevicius AR. 1998. Skeletal allometry and interlimb scaling patterns in mustelid carnivorans. *Journal of Morphology* **235:** 121–134.

Hildebrand M. 1977. Analysis of asymmetrical gaits. *Journal of Mammalogy* **58:** 131–156.

Hildebrand M, Goslow GE. 2001. *Analysis of vertebrate structure*, 5th edn. New York: John Wiley and Sons.

Holmes T. 1980. *Locomotor adaptations in the limb skeletons of North American mustelids*. MA thesis, Humboldt State University.

Koepfli KP, Wayne RK. 2003. Type I sts markers are more informative than cytochrome *b* in phylogenetic reconstruction of the Mustelidae (Mammalia: Carnivora). *Systematic Biology* **52:** 571–593.

Kurtén B, Anderson E. 1980. *Pleistocene mammals of North America*. New York: Columbia University Press.

Leach D. 1977a. The descriptive postcranial osteology of marten (*Martes Americana*. Turton) and fisher (*Martes pennati* Erxleben): the appendicular skeleton. *Canadian Journal of Zoology* **55:** 199–214.

Leach D. 1977b. The forelimb musculature of marten (*Martes americana* Turton) and fisher (*Martes pennati* Erxleben). *Canadian Journal of Zoology* **55:** 31–41.

MacLeod N, Rose KD. 1993. Inferring locomotor behavior in Paleogene mammals via eigenshape analysis. *American Journal of Science* **293-A:** 300–355.

Martin LD. 1989. Fossil history of the terrestrial Carnivora. In: Gittleman JL, ed. *Carnivore behavior, ecology and evolution*. New York: Cornell University Press, 536–568.

Maynard Smith J, Savage RJG. 1956. Some locomotory adaptations in mammals. *Journal of the Linnean Society* **42:** 603–622.

Nolte AW, Sheets HD. 2005. Shape based assignment tests suggest transgressive phenotypes in natural sculpin hybrids (Teleostei, Scorpaeniformes, Cottidae). *Frontiers in Zoology* **2:** 11–23.

Nowak R. 2000. *Walker's mammals of the world*. Baltimore: John Hopkins University. Press.

Pasitschniak-Arts M, Lariviére S. 1995. *Gulo gulo*. *Mammalian Species* **499:** 1–10.

Powell RA. 1981. *Martes pennanti*. *Mammalian Species* **156:** 1–6.

Quaife LR. 1978. *The form and function of the North American badger (Taxidea taxus) in relation to its fossorial way of life*. MSc thesis, University of Calgary.

Ray CE, Anderson E, Webb DS. 1981. The Blancan carnivore. *Trigonictis* (Mammalia: Mustelidae) in the eastern USA. *Brimleyana* **5:** 1–36.

Shimer HW. 1903. Adaptations to aquatic, arboreal, fossorial and cursorial habits in. Mammals. III fossorial adaptations. *American Naturalist* **37:** 819–825.

Simpson GG. 1945. The principles of classification and a classification of mammals. *Bulletin of the America Museum of Natural History.* **85:** 1–350.

Tarasoff FJ. 1972. Comparative aspects of the hindlimbs of the river otter, sea otter, and harp seal. In: Harrison RJ, ed. *Functional anatomy of mammals*. New York: Academic Press, 333–359.

Tarasoff FJ, Bisaillon A, Piérard J, Whitt AP. 1972. Locomotory patterns and external morphology of the river otter, sea otter and harp seal (Mammalia). *Canadian Journal of Zoology* **50:** 915–927.

Taylor ME. 1974. The functional anatomy of the forelimb of some African Viverridae (Carnivora). *Journal of Morphology* **143:** 307–336.

Taylor ME. 1976. The functional anatomy of the hindlimb of some African Viverridae (Carnivora). *Journal of Morphology* **148:** 227–254.

Taylor ME. 1989. Locomotor adaptations by carnivores. In: Gittleman JL, ed. *Carnivore behavior, ecology and evolution*. New York: Cornell University Press, 382–409.

Van Valkenburgh B. 1985. Locomotor diversity within past and present guilds of large predatory mammals. *Paleobiology* **11:** 406–428.

Van Valkenburgh B. 1987. Skeletal indicators of locomotor behavior in living and extinct carnivores. *Journal of Vertebrate Paleontology* **7:** 162–182.

Wagner H. 1976. A new species of *Pliotaxidea* (Mustelidae: Carnivora) from California. *Journal of Paleontology* **50:** 107–127.

Williams TM. 1983. Locomotion in the North American mink, a semi-aquatic mammal. II. The effect of an elongate body on running energetics and gait patterns. *Journal of Experimental Biology* **105:** 283–295.

Zakrzewski RL. 1967. The systematic position of *Canimartes*? from the upper Pliocene of Idaho. *Journal of Mammalogy*. **48:** 293–297.

Zelditch ML, Swiderski DL, Sheets HD, Fink WL. 2004. *Geometric morphometrics for biologists: a primer*. London: Elsevier Academic Press.

APPENDIX 1

Sample of recent and fossil musteloids. The number of elements for each species (*N*) is listed for the extant material. For the fossil material, each specimen is listed individually and the number of specimens per individual (*N*) is listed.

	Humerus *N*	Ulna *N*	Femur *N*	Tibia *N*
Extant species				
Eira barbara	12	12	11	12
Enhydra lutris	7	5	7	6
Galictis cuja	4	4	4	4
Galictis vittata	7	6	6	7
Gulo gulo	20	19	20	19
Lontra canadensis	14	15	16	16
Lutra lutra	13	13	13	13
Martes americana	14	13	14	13
Martes martes	13	13	13	13
Martes pennanti	15	15	15	15
Meles meles	16	15	13	10
Mephitis mephitis	17	17	17	16
Mustela erminea	26	25	28	24
Mustela frenata	29	28	30	30
Mustela nivalis	7	7	7	7
Mustela vison	18	18	19	20
Spilogale putorious	11	11	11	11
Taxidea taxus	19	19	19	19
Fossil specimens				
Unknown (USNM 2021416)	1	1		
Trigonictis macrodon (IMNH 482)	1	1		
Trigonictis cookii (IMNH 4934)	1			
Trigonictis sp. (IMNH 69008)	1			
Trigonictis cookii (UM 49819)	1	1	1	1
Trigonictis macrodon (UM 53554)	1			
Trigonictis macrodon (UM 53556)	1			
Trigonictis macrodon (UM 55001)	1			
Trigonictis macrodon (UM 51376)	1			
Trigonictis macrodon (UM 51049)	1			
Trigonictis cookii (UF 27510)	1			
Trigonictis cookii (IMNH 1100)		1		
Trigonictis cookii (IMNH 571)		1		
Mustelidae (UF 18087)		1		
Trigonictis sp. (HAFO 386)			1	
Trigonictis macrodon (UM 54683)			1	
Trigonictis macrodon (UF 14256)			1	
Trigonictis macrodon (UF 16762)			1	
Trigonictis sp. (HAFO 387)				1
Trigonictis macrodon (UM 56096)				1
Trigonictis macrodon (UF 18475)				1